

Spatially selective visible light photocatalytic activity of TiO₂/BiFeO₃ heterostructures

Yiling Zhang, Andrew M. Schultz, Paul A. Salvador and Gregory S. Rohrer*

Received 9th December 2010, Accepted 8th January 2011

DOI: 10.1039/c0jm04313c

Heterostructures of thin titania films on BiFeO₃ substrates were grown by pulsed laser deposition. The heterostructures, when excited by visible light with energies between 2.53 and 2.70 eV, photochemically reduce aqueous silver cations from solution in patterns that mimic the structure of the ferroelectric domains in the substrate. Under the same conditions, titania by itself reduces insignificant amounts of silver. The observations indicate that electrons generated in the substrate are influenced by dipolar fields in the ferroelectric domains and transported through the titania film to reduce silver on the surface.

1 Introduction

Titania is of interest for the photovoltaic conversion of light to electricity^{1,2} and the photocatalytic conversion of light to chemical fuels.^{3,4} One of the factors that limit the utility of titania for these applications is its band gap. Because the absorption edges of rutile and anatase are at about 3.0 eV and 3.2 eV, respectively, they absorb significant amounts of light only in the UV portion of the spectrum.^{5–7} The majority of the energy in the solar spectrum, on the other hand, is carried by photons with a lower energy. Therefore, titania absorbs only a small portion of the available solar energy. This limitation has motivated attempts to modify the absorption edge of titania so that it can absorb visible light.

One strategy is to substitute a portion of the oxygen with another electronegative atom. For example, N-doped TiO₂ powders and films have been shown to absorb visible light^{8–15} through electronic states that are approximately 0.75 eV above the valence band edge of pure titania.^{12,15} S-doping,^{9,13,16–19} C-doping,^{9,19–22} and F-doping²³ have also been reported to increase visible light absorption in TiO₂. Codoping by S and C have been reported²⁴ and N, C and N, F codoped materials have been reported to exhibit superior visible light activity when compared to materials doped with a single element.^{25,26}

A second strategy is to replace a portion of the titanium with another metal atom. Fe is the most commonly used additive that induces visible light absorption.^{27–30} Cr-doping,^{27,31} V-doping,^{27,32} Mo-doping,³³ Sb–Cr-codoping,³⁴ and Fe–N-codoping³⁵ have also been reported. In general, this doping increases the photocatalytic activity of TiO₂ in the 400–600 nm range. As with doping on the anion site, it is frequently reported

that the substitutional elements create new electronic levels within titania's band gap, thereby increasing visible light absorption. However, the introduction of substitutional elements also creates scattering centers and this can cause a decrease in the photochemical activity. For example, it has been reported that substitutional Fe serves as a center for charge carrier recombination.^{29,36}

Another way to increase the visible light activity of titania is through the addition of an adsorbed molecular species that can absorb visible light and donate an electron or hole to the titania. There is an extensive literature on the use of organic dyes for this purpose.^{1,2,36} It is also possible to use inorganic ions, such as Ce³⁺/Ce⁴⁺, to shuttle electrons and holes to and from titania.^{37,38}

It has recently been reported that titania supported on a visible light absorbing core of FeTiO₃ shows enhanced visible light photoactivity.³⁹ This particular scheme for inducing visible light activity in titania has the advantage of presenting a pure, undoped titania surface at a solid–liquid interface that is not covered by extrinsic adsorbates. The present work takes this approach to inducing visible light activity in titania, but uses a ferroelectric substrate (BiFeO₃) that also has internal dipolar fields that will separate charge carriers and may reduce recombination.

BiFeO₃ is a semiconductor with a relatively narrow band gap of about 2.5 eV.^{40–42} It has also been reported to be photocatalytically active in visible light.^{43,44} Of importance for the present study, it is ferroelectric with spontaneous polarization along the pseudo-cubic <111> directions of 6.1 μC cm⁻².⁴⁵ Spontaneous polarization in the ferroelectric domains leads to band bending that transports photogenerated electrons and holes in opposite directions^{46–48} and this can lead to spatially resolved reactivity.^{49–51} Because the photogenerated carriers are separated by the internal polarization, they are less likely to recombine and this may enhance photocatalytic efficiency. It has recently been shown that charge separation occurs within titania/BaTiO₃

Department of Materials Science and Engineering, Carnegie Mellon University, Pittsburgh, PA, USA. E-mail: gr20@andrew.cmu.edu; Fax: +1 412 268 7596; Tel: +1 412 268 2696

heterostructures when illuminated by UV light.^{49,52–54} The separation of carriers leads to the separation of the reduction and oxidation half reactions so that the back reaction of intermediates is also suppressed. Similar effects have been observed for BiFeO₃ illuminated by UV light.⁵⁵

The purpose of this paper is to show that titania can be made photochemically active in visible light with a wavelength of 460 nm by supporting it on a BiFeO₃ substrate. This is demonstrated by the reduction of aqueous silver cations to silver metal. Furthermore, the reduction reaction is spatially selective and correlated to the domains in the BiFeO₃ substrate. The reactivity of the titania film decreases as the film thickness increases. When titania is not supported by BiFeO₃, illumination by the 460 nm source yields an amount of photochemically reduced silver that is not significant. Based on these observations, it is concluded that electrons generated in the BiFeO₃ travel through the titania film to participate in reactions at the solid–liquid interface.

2 Experimental details

Polycrystalline samples of BiFeO₃ were synthesized from Bi₂O₃ (Alfa Aesar 99.99%) and Fe₂O₃ (Alfa Aesar 99.945%) powders. Stoichiometric mixtures of Bi₂O₃ and Fe₂O₃ were ball milled in ethanol for 18–24 h and then dried at 85 °C. The dried powders were placed in an alumina crucible and calcined at 700 °C for 3 h in air. The powder was again ball milled in ethanol for 24 h, dried, and uniaxially compressed in a cylindrical die with a load of 105 MPa to form samples approximately 1 cm in diameter and 3 mm thick. The pellets were sintered at 850 °C for 3 h. After this procedure, X-ray diffraction indicated that the majority phase was BiFeO₃. Small amounts of Bi₂Fe₄O₉, Bi₂₅FeO₄₀, and Fe₂O₃ were also detected in the diffraction pattern and will be referred to collectively in the remainder of the manuscript as minority phases. To prepare the surfaces for analysis, the sintered pellets were lapped flat with an aqueous Al₂O₃ suspension (9 μm or 3 μm, Logitech) and then polished with a 0.02 μm colloidal SiO₂ suspension (Mastermet 2, Buehler) using a Logitech polisher. The polished pellets were thermally etched at 600 °C for 3 h to repair the polishing damage. For two control experiments, similar procedures, described previously, were used to prepare polycrystalline BaTiO₃⁵¹ and TiO₂.⁵⁶

Pulsed laser deposition (PLD) was used to deposit TiO₂ films on BiFeO₃, BaTiO₃, and single crystal SrTiO₃ (100) (MTI Corporation, USA). The TiO₂ target was prepared by compressing TiO₂ powder uniaxially in a cylindrical die under a load of 75 MPa to form a disc shaped sample with a diameter of approximately 2.5 cm. The target was then sintered in an alumina crucible at 1400 °C for 12 h. For one of the control experiments, an Fe-doped titania target (2 at% Fe) was prepared using the same procedure, but adding the appropriate amount of Fe₂O₃ as an iron source. A KrF (λ = 248 nm) laser was pulsed at 3 Hz with an energy density of 2 J cm⁻². The target-to-substrate distance was maintained ~6 cm during the growth of all films. A base pressure of ~10⁻⁵ Torr was established in the chamber with the sample at 120 °C. The sample was then heated to a nominal temperature of 500 to 700 °C at a rate of 25 °C min⁻¹. Because the surface of the substrate is lower than the nominal temperature, and depends on thermal conductivity through the sample, films on thin substrates were grown at 500 °C and films on thicker ones

were grown at 700 °C. A flow of O₂ was maintained at 5 mTorr during heating and deposition. After heating, the TiO₂ target surface was cleaned by laser ablation at 3 Hz for 10 min. To determine the deposition rate, a TiO₂ film was deposited on a LaAlO₃ single crystal using 3000 laser pulses. The thickness of TiO₂ film was then measured by X-ray reflectivity and the rate was determined to be ~0.0067 nm per pulse. TiO₂ was deposited using 1500, 3000, and 12 000 pulses, to produce films with estimated thicknesses of 10, 20, and 80 nm, respectively. After deposition, the samples were cooled in a static atmosphere of 5 Torr O₂ at a rate of 25 °C min⁻¹. Consistent with a recent study of titania films on BaTiO₃,⁵⁷ electron backscatter diffraction measurements indicate that both rutile and anatase are grown, that different grains promote the growth of films with different phases and orientations, and that the phase and orientation are uniform on each BiFeO₃ grain. The use of bulk BiFeO₃ substrates eliminates the possibility of domain orientation constraints that occur in BiFeO₃ thin films and superlattices.^{58,59}

The photochemical reduction of silver was used as a marker reaction to test for photoactivity. The reaction leaves silver deposits on the surface that can be observed by microscopy.^{60,61} For these reactions, a 0.115 M AgNO₃ solution was prepared by dissolving AgNO₃ in de-ionized H₂O. A viton O-ring was placed on the sample and filled with AgNO₃ solution. A quartz cover slip was placed on top of the O-ring and held in place by the surface tension of the liquid. The reaction assembly was brought as close as possible to a blue LED with an emission energy of 2.53 to 2.70 eV (LUXEON, Philips), which was operated at 750 mA and 4.0 V. After illuminating the sample for 60 s, the O-ring and the quartz slip were removed, and the samples were rinsed by sequential immersion in two baths of de-ionized H₂O, and then dried using a stream of clean nitrogen. By using energy dispersive spectroscopy in a scanning electron microscope, it was confirmed that the reaction product left on the surface contained silver. X-Ray diffraction of a sample illuminated for several hours (to increase the amount of reaction product) confirmed that metallic silver had been formed, consistent with previous findings.^{60,61} Although the oxidation half reaction was not examined in these experiments, the continuous accumulation of silver with longer illumination indicates that the holes do not accumulate and the eventual appearance of macroscopically observable gaseous bubbles in the silver nitrate solution is consistent with oxygen production.

Atomic force microscopy (AFM) was used to characterize the surfaces of the samples. Images were recorded using an NTegra (NT-MDT) microscope or a Dimension 3100 (Veeco) microscope. Topographic images of the surfaces were taken in conventional semi-contact mode before and after Ag⁺ reduction reactions for comparison. The images were analyzed to estimate average local Ag thicknesses precipitated on the surfaces. Piezoresponse force microscopy (PFM) images of BiFeO₃ substrates were taken before and after TiO₂ film deposition to determine the positions of the ferroelectric domains.

3 Results

The heterostructures considered here consist of either rutile/BiFeO₃ or anatase/BiFeO₃. Therefore, we begin by evaluating the photochemical activity of each of the three phases by

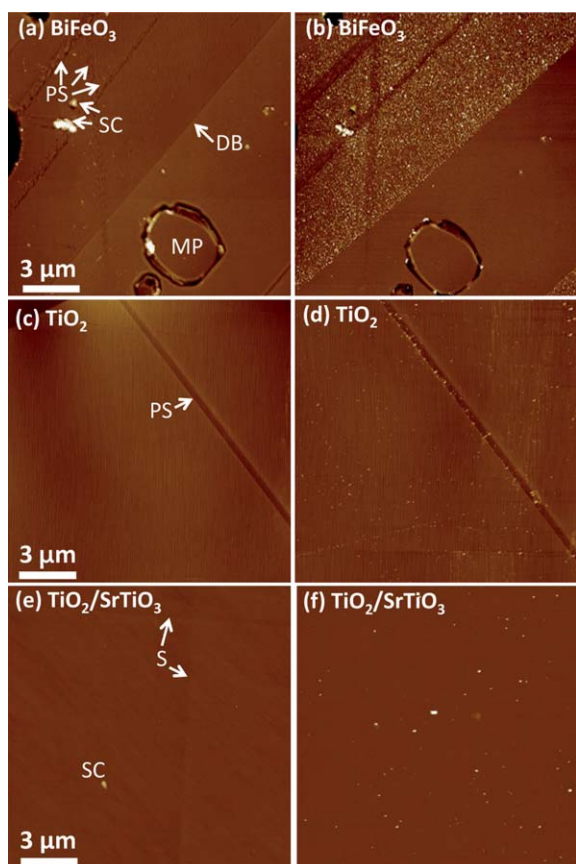


Fig. 1 AFM topographic images of surfaces of (a) bare BiFeO₃ before reaction, (b) BiFeO₃ after reaction, (c) bare rutile TiO₂ before reaction, (d) rutile TiO₂ after reaction, (e) 20 nm anatase TiO₂ film on SrTiO₃ (100) before reaction, (f) 20 nm anatase TiO₂ film on SrTiO₃ (100) after reaction. The topographic contrast in all images is 100 nm from bright to dark.

themselves. The AFM images in Fig. 1 show the surface of BiFeO₃ (a,b), rutile (c,d), and anatase (e,f). The BiFeO₃ and rutile are bulk ceramic materials. The anatase sample, on the other hand, is a 20 nm film deposited on SrTiO₃ (100) under conditions that produce anatase (001).^{62,63} The topographic contrast in the AFM images arises from a variety of sources including surface steps (S), residual polishing scratches (PS), boundaries between ferroelectric domains (DB), surface contamination (SC), and inclusions of minority phases (MP), which are labeled on the micrographs. After the photochemical reaction, the surfaces of certain domains in BiFeO₃ are coated with reduced silver (white contrast). The heights of these features vary between 20 and 130 nm. This is the same reaction that has been observed previously on titania,^{56,64} BaTiO₃,^{50,51} and PZT^{65,66} when illuminated by UV light. Here, the reaction is initiated by visible light. On the titania surfaces, only small changes in the contrast are found, corresponding either to a small amount of silver or surface contamination from immersion in the silver nitrate solution. Based on these images, it can be concluded that the BiFeO₃ surface reduced far more silver on the active domains than either of the titania surfaces.

The images in Fig. 2 show the correlation between the piezoresponse of the substrate (a) and heterostructure (b) and the

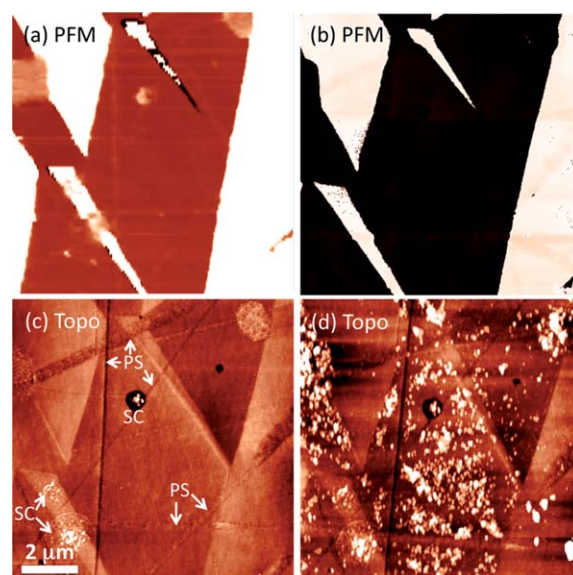


Fig. 2 (a) PFM phase image of bare BiFeO₃ surface. (b) PFM phase image of 10 nm TiO₂/BiFeO₃. (c) Topographic image of 10 nm TiO₂/BiFeO₃ before reaction. (d) Topographic image of 10 nm TiO₂/BiFeO₃ after reaction. PFM phase contrast scale is -180° to 180° from bright to dark. Topographic contrast scale is 15 nm from bright to dark.

photochemical reactivity of the titania film surface (c and d). The contrast in the piezoresponse force microscopy (PFM) phase image of the BiFeO₃ surface reveals the domain structure of the substrate. After depositing a 10 nm titania film, the piezoresponse of the heterostructure is the same. Therefore, the displacements in the substrate that create the PFM signal are not significantly affected by the 10 nm titania film. The image in Fig. 2(c) shows the topography of the film surface. Note that some of the components of the film topography correlate exactly with the domain structure revealed by the PFM images. After the sample is illuminated by blue light in the silver nitrate solution, new contrast appears on the surface, corresponding to reduced silver (see Fig. 2(d)). Similar to the reaction on the bare substrate (Fig. 1(b)), there is more silver reduced on some domains than others. A typical height for the silver is 100 nm. In this case, the domains that are dark in the PFM images reduce more silver than the light contrast domains.

Because the substrate and the thin titania film are able to reduce Ag with visible light, but titania by itself can not, it is reasonable to assume that as the film increases in thickness, it will become less reactive. To test this idea, the experiment was repeated using titania films that were 20 nm and 80 nm thick and the results are compared in Fig. 3. For each case, one test line is drawn on the image recorded before the reaction and a second is drawn on the same location after the reaction. The topography along these two lines is compared in the third panel of the figure. For the 10 nm and 20 nm thick films, the maximum heights of the deposited silver are in the range of 60 to 100 nm, but for the 80 nm thick titania film, the heights of the deposited silver do not exceed 20 nm. For comparison, the maximum height of silver deposited on the bare BiFeO₃ surface under the same conditions is approximately 130 nm. Therefore, the amount of silver reduced by the titania film decreases with film thickness.

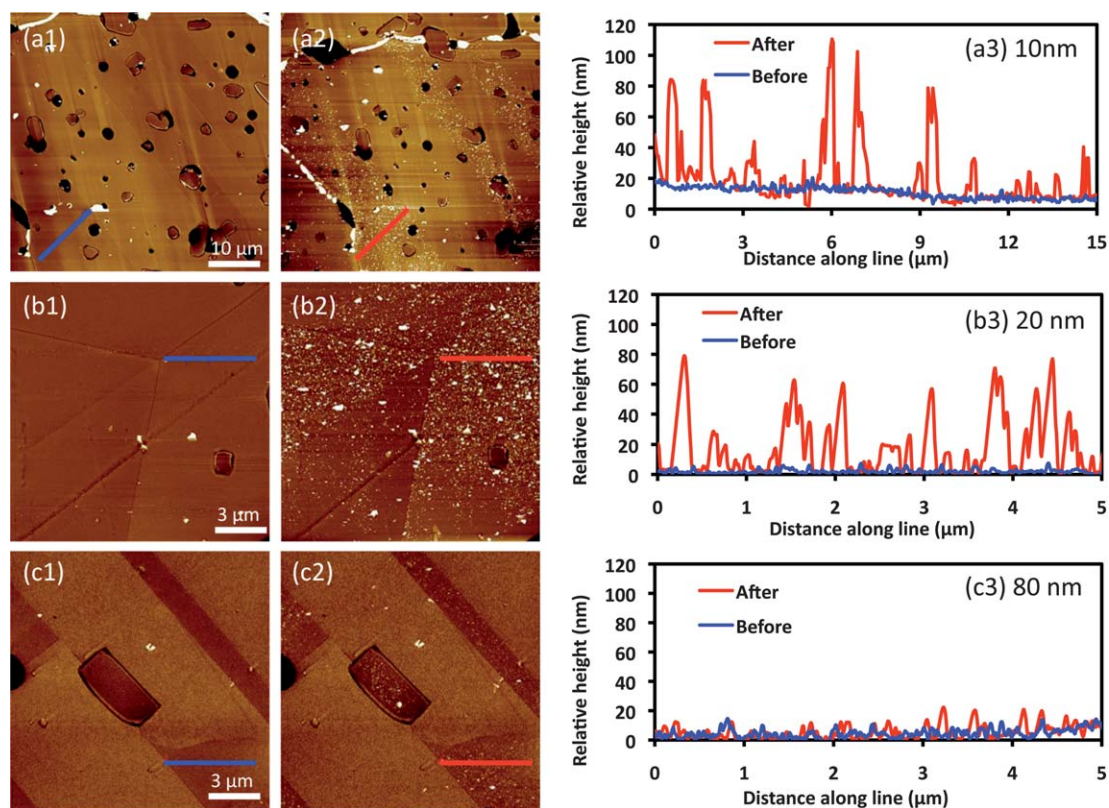


Fig. 3 AFM topographic images and height profiles of TiO₂/BiFeO₃ with TiO₂ thickness of (a) 10, (b) 20, and (c) 80 nm. Each row from left to right shows the image before reaction, the image after reaction, and a comparison of the height profiles at the same locations. The contrast scale from bright to dark is 100 nm for all images.

Ideally, the only component of the heterostructures that can absorb light and create carriers is the substrate. However, based on previous work,⁶⁷ one could hypothesize that Fe contamination (which could diffuse from the BiFeO₃ substrate during growth) might increase absorption in the film. While it is impossible to eliminate contamination from the substrate, it is possible to grow an Fe-doped titania film on a substrate that does not absorb visible light, to see if Fe-doping in the film by itself is sufficient to explain the visible light activity observed in the TiO₂/BiFeO₃ heterostructures. The AFM images in Fig. 4 compare the surface of a 10 nm thick Fe-doped titania film on SrTiO₃ (100) before and after the reaction. It is clear from the image in

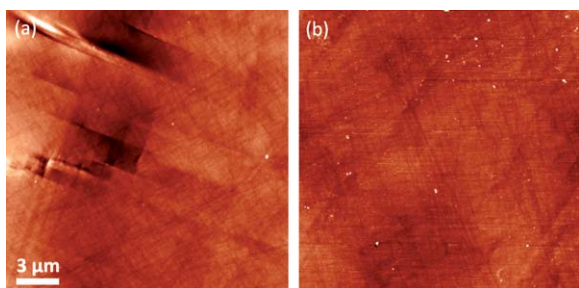


Fig. 4 Topographic images of a 10 nm thick Fe-doped-TiO₂ film on SrTiO₃ (100) (a) before reaction and (b) after reaction. The contrast scale from bright to dark is 15 nm. The images are not from the same area, but are representative of all areas that were imaged.

Fig. 4(b) that very little silver is deposited on the Fe-doped titania film. Therefore, Fe-doping in the titania layer is not sufficient to explain the reactivity of the unintentionally doped titania films on the BiFeO₃ surface.

It is also feasible that the ferroelectric substrate creates charged interface states that induce the visible light activity. To test this idea, a 20 nm titania film was grown on BaTiO₃, which is also ferroelectric, but does not absorb visible light.^{68,69} The results are shown in Fig. 5. The image in Fig. 5(a) shows the surface of the titania film before reaction. The image shows some weak contrast that arises from the domain structure of the substrate. The image in Fig. 5(b) shows some silver on the surface. However, the amount of deposited silver is much less

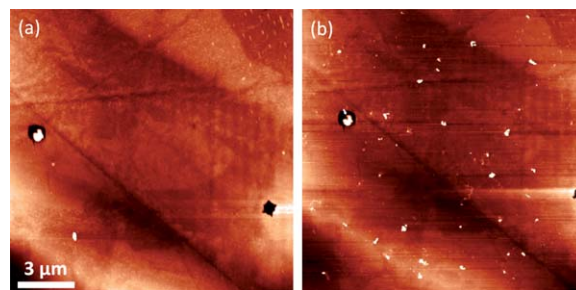


Fig. 5 Topographic images of a 20 nm TiO₂ film on BaTiO₃ (a) before reaction and (b) after reaction. The contrast scale from bright to dark is 40 nm.

than on films supported by BiFeO₃ and similar to the silver observed on the surface of bulk titania (see Fig. 1). Furthermore, there is no obvious correlation between the pattern of silver and the underlying domain structure as observed when the same structure is illuminated by UV light.^{49,53}

4 Discussion

The results presented here indicate that the photochemical reduction of silver, initiated by visible light, is spatially selective on the BiFeO₃ surface. While the amount of silver was observed to vary somewhat with the grain and orientation, similar spatially selective reactivity was found on all grains. Assuming the spatially selective reactivity is analogous to what occurs in BaTiO₃ and PZT, then the reduction reaction is probably associated with domains that have polarizations pointed away from the surface, where bands are bent downward and electrons move down the gradient toward the surface.^{49–51,66} The main difference is that for BaTiO₃ and PZT, the same reaction can only be initiated by UV light.

Titania is relatively unreactive when illuminated by visible light. The images of bulk rutile (Fig. 1(d)), anatase supported by SrTiO₃ (Fig. 1(f)), and titania supported by BaTiO₃ (Fig. 5(b)) after illumination suggest that a small amount of silver is reduced, even though the band gaps are larger than the energy of illumination. The distribution of reaction product is inhomogeneous; we assume that the carriers responsible for this limited reaction are generated by absorption of light at defect states such as oxygen vacancies that have states below the conduction band edge. This background reactivity is presumably present in all of the experiments, but is overwhelmed by the spatially selective reactivity of the films supported by BiFeO₃.

The observations from the TiO₂/BiFeO₃ heterostructures indicate that the carriers that react on the titania film surface are created by absorption in the substrate. This is completely analogous to the conclusion reached by Burbure *et al.*^{49,53} in studies of thin titania films on BaTiO₃ excited by UV radiation. One observation that supports this conclusion is that when titania is not supported by BiFeO₃, it absorbs very little light of this energy and does not reduce significant amounts of silver. The second observation is that the patterns of silver on the surface have the same configuration as those in the supporting substrate. The third supporting observation is that the reactivity of the film decreases as the thickness increases. This all indicates that light absorbed in the narrower band gap substrate creates electrons and holes that travel through the thin film and react on the surface.

It should be mentioned that a recent study of anatase–BiFeO₃ nanocomposites demonstrated enhanced visible light activity compared to titania alone.⁶⁷ In that case, the enhancement was attributed to interdiffusion of the metallic components and, in particular, Fe-doping of the titania. However, the results shown in Fig. 4 indicate that Fe-doping in the film is, by itself, not sufficient to make the films significantly more reactive in the conditions used here. Another possible explanation is that multiple reflections and scattering at the buried interface between the ferroelectric and the supported film enhance the path length of light in the titania film and lead to enhanced absorption. However, if this were the case, then we would have expected the

same result in the film supported by BaTiO₃; the film supported by BaTiO₃ is not significantly more reactive in visible light than bulk titania.

Of the situations examined here, the BiFeO₃ substrate had the highest reactivity and the titania films all have lower reactivities. If the goal were only to have the highest reactivity for silver reduction, BiFeO₃ would be the best choice. However, to be useful for water photolysis, the material must be stable in aqueous solutions and its conduction band energy must be higher than the hydrogen reduction level. While these two conditions are met by titania, they are not met by BiFeO₃.

To understand the mechanism of visible light reactivity, plausible energy level diagrams for the heterostructures (see Fig. 6) are constructed according to the following principles. First, BiFeO₃ is reported to be a p-type semiconductor^{70,71} and its band gap has been reported to be between 2.2 and 2.7 eV in different studies.^{40–42} Here, we will assume a value of 2.5 eV. The electron affinity is estimated to be 4.6 eV using the method described by Morrison.⁷² The position of the Fermi level is

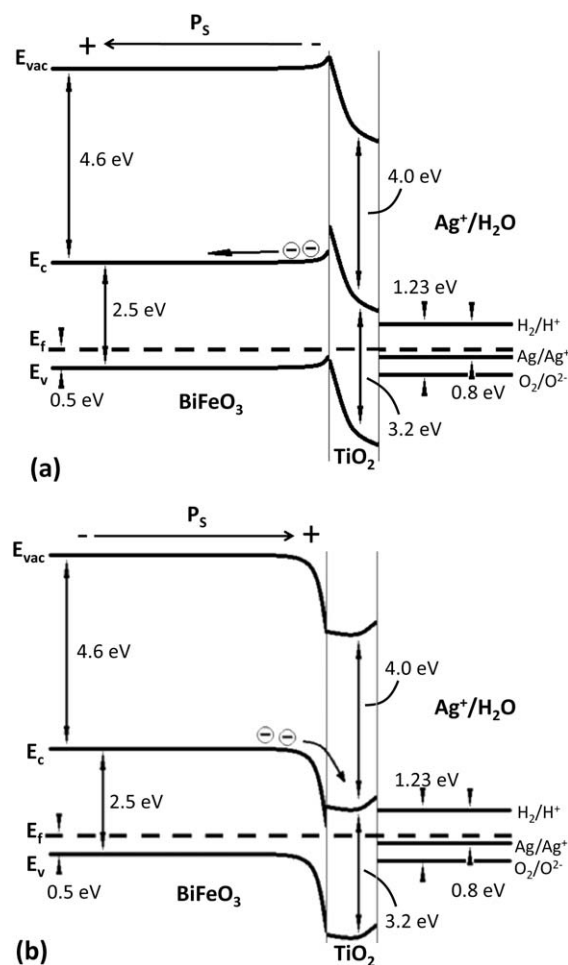


Fig. 6 Schematics of band structure of BiFeO₃/TiO₂/H₂O with the polarization (P_s) of BiFeO₃ (a) pointing away from BiFeO₃/TiO₂ interface, and (b) pointing towards BiFeO₃/TiO₂ interface. In the figure, the vacuum level, conduction band edge, Fermi level and valence band edge are given by the symbols E_{vac} , E_c , E_f , and E_v , respectively. The hydrogen, silver, and oxygen redox levels are indicated on the right.

estimated to be 0.5 eV above the top of the valence band edge. Undoped TiO₂ is typically oxygen-deficit and thus is considered n-type with a band gap of 3.0 eV (for rutile)^{5,6} and 3.2 eV (for anatase).⁷ The work function is reported to be 4.2 eV⁷³ and the Fermi level is approximately 0.2 eV below the bottom of the conduction band.⁵ When titania is supported by BiFeO₃, a p–n junction is created. When bulk TiO₂ is in contact with the solution, exchange of charge with the solution leads to upward band bending at the interface. However, because the film thickness is less than the expected depletion layer (~100 nm), the band is not expected to be able to relax to the bulk level.⁷⁴ Assuming that the energy levels at the interface are strongly influenced by the polarization, then the bands in BiFeO₃ bend upward when the polarization is directed away from the surface (referred to as negative domains) and downward when directed toward the surface (positive domains), as shown in Fig. 6(a) and (b), respectively. Therefore, photogenerated electrons in negative domains encounter a barrier that prevents them from reaching the surface. This is consistent with the observation that no silver is reduced above negative domains. In positive domains, the opposite is true; electrons are driven to the interface. In this case the electrons have energies above the conduction band edge and can continue directly to the solid–liquid interface and reduce silver cations, as observed in the experiment. Assuming this mechanism is correct, then the same mechanism should apply to other heterostructures where titania is supported by a narrow band gap, p-type substrate.

5 Conclusions

Thin titania films supported on BiFeO₃ substrates reduce silver cations from aqueous solutions when excited by visible light with an energy less than titania's band gap. The patterns of reduced silver on the titania surface mimic the structure of the domains found in the BiFeO₃ substrate. The observations indicate that electrons generated in the BiFeO₃ substrate can be transported to the surface of the film where they reduce silver. Electron transport to the surface is favored in domains with a positive polarization pointed toward the surfaces and inhibited in domains with the opposite polarization.

Acknowledgements

The work was supported by National Science foundation grant DMR 0804770.

References

- 1 B. O'Regan and M. Gratzel, *Nature*, 1991, **353**, 737–740.
- 2 F. Sauvage, D. H. Chen, P. Comte, F. Z. Huang, L. P. Heiniger, Y. B. Cheng, R. A. Caruso and M. Gratzel, *ACS Nano*, 2010, **4**, 4420–4425.
- 3 A. Fujishima and K. Honda, *Nature*, 1972, **238**, 37–38.
- 4 F. E. Osterloh, *Chem. Mater.*, 2008, **20**, 35–54.
- 5 R. G. Breckenridge and W. R. Hosler, *Phys. Rev.*, 1953, **91**, 793–802.
- 6 J. Pascual, J. Camassel and H. Mathieu, *Phys. Rev. B*, 1978, **18**, 5606–5614.
- 7 H. Tang, F. Levy, H. Berger and P. E. Schmid, *Phys. Rev. B: Condens. Matter*, 1995, **52**, 7771–7774.
- 8 R. Asahi, T. Morikawa, T. Ohwaki, K. Aoki and Y. Taga, *Science*, 2001, **293**, 269–271.
- 9 X. B. Chen and C. Burda, *J. Am. Chem. Soc.*, 2008, **130**, 5018–5019.
- 10 J. L. Gole, J. D. Stout, C. Burda, Y. B. Lou and X. B. Chen, *J. Phys. Chem. B*, 2004, **108**, 1230–1240.
- 11 T. Morikawa, R. Asahi, T. Ohwaki, K. Aoki and Y. Taga, *Jpn. J. Appl. Phys.*, 2001, **40**, L561–L563.
- 12 R. Nakamura, T. Tanaka and Y. Nakato, *J. Phys. Chem. B*, 2004, **108**, 10617–10620.
- 13 K. Nishijima, B. Ohtani, X. L. Yan, T. Kamai, T. Chiyoya, T. Tsubota, N. Murakami and T. Ohno, *Chem. Phys.*, 2007, **339**, 64–72.
- 14 Y. Sakatani, J. Nunoshige, H. Ando, K. Okusako, H. Koike, T. Takata, J. N. Kondo, M. Hara and K. Domen, *Chem. Lett.*, 2003, 1156–1157.
- 15 S. Sakthivel, M. Janczarek and H. Kisch, *J. Phys. Chem. B*, 2004, **108**, 19384–19387.
- 16 W. K. Ho, J. C. Yu and S. C. Lee, *J. Solid State Chem.*, 2006, **179**, 1171–1176.
- 17 H. X. Li, X. Y. Zhang, Y. N. Huo and J. Zhu, *Environ. Sci. Technol.*, 2007, **41**, 4410–4414.
- 18 T. Ohno, M. Akiyoshi, T. Umebayashi, K. Asai, T. Mitsui and M. Matsumura, *Appl. Catal., A*, 2004, **265**, 115–121.
- 19 T. Tachikawa, S. Tojo, K. Kawai, M. Endo, M. Fujitsuoka, T. Ohno, K. Nishijima, Z. Miyamoto and T. Majima, *J. Phys. Chem. B*, 2004, **108**, 19299–19306.
- 20 H. Irie, Y. Watanabe and K. Hashimoto, *Chem. Lett.*, 2003, 772–773.
- 21 J. H. Park, S. Kim and A. J. Bard, *Nano Lett.*, 2006, **6**, 24–28.
- 22 M. Shen, Z. Y. Wu, H. Huang, Y. K. Du, Z. G. Zou and P. Yang, *Mater. Lett.*, 2006, **60**, 693–697.
- 23 D. Li, N. Ohashi, S. Hishita, T. Kolodiazhnyi and H. Haneda, *J. Solid State Chem.*, 2005, **178**, 3293–3302.
- 24 T. Ohno, T. Tsubota, M. Toyofuku and R. Inaba, *Catal. Lett.*, 2004, **98**, 255–258.
- 25 D. M. Chen, Z. Y. Jiang, J. Q. Geng, Q. Wang and D. Yang, *Ind. Eng. Chem. Res.*, 2007, **46**, 2741–2746.
- 26 D. Li, H. Haneda, S. Hishita and N. Ohashi, *Chem. Mater.*, 2005, **17**, 2596–2602.
- 27 N. Serpone, D. Lawless, J. Disdier and J. M. Herrmann, *Langmuir*, 1994, **10**, 643–652.
- 28 S. Nahar, K. Hasegawa and S. Kagaya, *Chemosphere*, 2006, **65**, 1976–1982.
- 29 X. H. Wang, J. G. Li, H. Kamiyama, Y. Moriyoshi and T. Ishigaki, *J. Phys. Chem. B*, 2006, **110**, 6804–6809.
- 30 W. J. Zhang, Y. Li, S. L. Zhu and F. H. Wang, *Chem. Phys. Lett.*, 2003, **373**, 333–337.
- 31 A. Ghicov, B. Schmidt, J. Kunze and P. Schmuki, *Chem. Phys. Lett.*, 2007, **433**, 323–326.
- 32 S. Klosek and D. Raftery, *J. Phys. Chem. B*, 2001, **105**, 2815–2819.
- 33 V. Stengl and S. Bakardjieva, *J. Phys. Chem. C*, 2010, **114**, 19308–19317.
- 34 H. Kato and A. Kudo, *J. Phys. Chem. B*, 2002, **106**, 5029–5034.
- 35 Y. Cong, J. L. Zhang, F. Chen, M. Anpo and D. N. He, *J. Phys. Chem. C*, 2007, **111**, 10618–10623.
- 36 W. J. Youngblood, S. H. A. Lee, K. Maeda and T. E. Mallouk, *Acc. Chem. Res.*, 2009, **42**, 1966–1973.
- 37 E. A. Kozlova, T. P. Korobkina and A. V. Vorontsov, *Int. J. Hydrogen Energy*, 2009, **34**, 138–146.
- 38 E. A. Kozlova, T. P. Korobkina, A. V. Vorontsov and V. N. Parmon, *Appl. Catal., A*, 2009, **367**, 130–137.
- 39 B. Gao, Y. J. Kim, A. K. Chakraborty and W. I. Lee, *Appl. Catal., B*, 2008, **83**, 202–207.
- 40 S. R. Basu, L. W. Martin, Y. H. Chu, M. Gajek, R. Ramesh, R. C. Rai, X. Xu and J. L. Musfeldt, *Appl. Phys. Lett.*, 2008, **92**, 091905.
- 41 T. Choi, S. Lee, Y. J. Choi, V. Kiryukhin and S. W. Cheong, *Science*, 2009, **324**, 63–66.
- 42 F. Gao, Y. Yuan, K. F. Wang, X. Y. Chen, F. Chen and J. M. Liu, *Appl. Phys. Lett.*, 2006, **89**, 102506.
- 43 C. M. Cho, J. H. Noh, I. S. Cho, J. S. An, K. S. Hong and J. Y. Kim, *J. Am. Ceram. Soc.*, 2008, **91**, 3753–3755.
- 44 F. Gao, X. Y. Chen, K. B. Yin, S. Dong, Z. F. Ren, F. Yuan, T. Yu, Z. Zou and J. M. Liu, *Adv. Mater.*, 2007, **19**, 2889–2892.
- 45 J. R. Teague, R. Gerson and W. J. James, *Solid State Commun.*, 1970, **8**, 1073–1074.
- 46 P. S. Brody, *Solid State Commun.*, 1973, **12**, 673–676.
- 47 P. S. Brody, *J. Solid State Chem.*, 1975, **12**, 193–200.
- 48 V. M. Fridkin, *Ferroelectrics*, 1984, **53**, 169–187.

-
- 49 A. Bhardwaj, N. V. Burbure, A. Gamalski and G. S. Rohrer, *Chem. Mater.*, 2010, **22**, 3527–3534.
- 50 J. L. Giocondi and G. S. Rohrer, *J. Phys. Chem. B*, 2001, **105**, 8275–8277.
- 51 J. L. Giocondi and G. S. Rohrer, *Chem. Mater.*, 2001, **13**, 241–242.
- 52 N. V. Burbure, P. A. Salvador and G. S. Rohrer, *J. Am. Ceram. Soc.*, 2006, **89**, 2943–2945.
- 53 N. V. Burbure, P. A. Salvador and G. S. Rohrer, *Chem. Mater.*, 2010, **22**, 5823–5830.
- 54 N. V. Burbure, P. A. Salvador and G. S. Rohrer, *Chem. Mater.*, 2010, **22**, 5831–5837.
- 55 N. V. Burbure, *Influence of Ferroelectric Substrates on the Photochemical Reactivity of TiO₂ Thin Films*, Carnegie Mellon University, 2009.
- 56 J. B. Lowekamp, G. S. Rohrer, P. A. M. Hotsenpiller, J. D. Bolt and W. E. Farneth, *J. Phys. Chem. B*, 1998, **102**, 7323–7327.
- 57 N. V. Burbure, P. A. Salvador and G. S. Rohrer, *J. Am. Ceram. Soc.*, 2010, **93**, 2530–2533.
- 58 H. W. Jang, S. H. Baek, D. Ortiz, C. M. Folkman, R. R. Das, Y. H. Chu, P. Shafer, J. X. Zhang, S. Choudhury, V. Vaithyanathan, Y. B. Chen, D. A. Felker, M. D. Biegalski, M. S. Rzechowski, X. Q. Pan, D. G. Schlom, L. Q. Chen, R. Ramesh and C. B. Eom, *Phys. Rev. Lett.*, 2008, **101**, 4.
- 59 R. Ranjith, R. V. K. Mangalam, P. Boullay, A. David, M. B. Lepetit, U. Luders, W. Prellier, A. Da Costa, A. Ferri, R. Desfeux, G. Vincze, Z. Radi and C. Aruta, *Appl. Phys. Lett.*, 2010, **96**, 022902.
- 60 W. C. Clark and A. G. Vondjidi, *J. Catal.*, 1965, **4**, 691–696.
- 61 J. M. Herrmann, J. Disdier and P. Pichat, *J. Catal.*, 1988, **113**, 72–81.
- 62 C. C. Hsieh, K. H. Wu, J. Y. Juang, T. M. Uen, J. Y. Lin and Y. S. Gou, *J. Appl. Phys.*, 2002, **92**, 2518–2523.
- 63 S. Yamamoto, T. Sumita, T. Yamaki, A. Miyashita and H. Naramoto, *J. Cryst. Growth*, 2002, **237**, 569–573.
- 64 P. A. M. Hotsenpiller, J. D. Bolt, W. E. Farneth, J. B. Lowekamp and G. S. Rohrer, *J. Phys. Chem. B*, 1998, **102**, 3216–3226.
- 65 S. Dunn, P. M. Jones and D. E. Gallardo, *J. Am. Chem. Soc.*, 2007, **129**, 8724–8728.
- 66 D. Tiwari and S. Dunn, *J. Mater. Sci.*, 2009, **44**, 5063–5079.
- 67 S. Li, Y. H. Lin, B. P. Zhang, J. F. Li and C. W. Nan, *J. Appl. Phys.*, 2009, 105.
- 68 L. Hafid, G. Godefroy, A. Elidrissi and F. Michelcalendini, *Solid State Commun.*, 1988, **66**, 841–845.
- 69 S. H. Wemple, *Phys. Rev. B: Solid State*, 1970, **2**, 2679–2689.
- 70 B. Vengalis, J. Devenson, A. K. Oginskis, R. Butkute, A. Maneikis, A. Steikonienė, L. Dapkus, J. Banys and M. Kinka, *Acta Phys. Pol., A*, 2008, **113**, 1095–1098.
- 71 H. Yang, H. M. Luo, H. Wang, I. O. Usov, N. A. Suvorova, M. Jain, D. M. Feldmann, P. C. Dowden, R. F. DePaula and Q. X. Jia, *Appl. Phys. Lett.*, 2008, **92**, 102113.
- 72 S. R. Morrison, *Electrochemistry at Semiconductor and Oxidized Metal Electrodes* Plenum Press, New York, 1980.
- 73 A. Imanishi, E. Tsuji and Y. Nakato, *J. Phys. Chem. C*, 2007, **111**, 2128–2132.
- 74 W. J. Albery and P. N. Bartlett, *J. Electrochem. Soc.*, 1984, **131**, 315–325.